

Molecular design and biological activity of potent and selective protein kinase inhibitors related to balanol

Kazunori Koide¹, Mark E Bunnage², Luigi Gomez Paloma², Joan R Kanter³, Susan S Taylor¹, Laurence L Brunton^{3*} and K C Nicolaou^{1,2*}

¹Department of Chemistry and Biochemistry, University of California, San Diego, 9500 Gilman Drive, La Jolla, CA 92093, USA, ²Department of Chemistry, The Scripps Research Institute, 10666 North Torrey Pines Road, La Jolla, CA 92037, USA and ³Departments of Pharmacology and Medicine, University of California, San Diego, 9500 Gilman Drive, La Jolla, CA 92093-0636, USA

Background: The protein kinase C (PKC) family of serine/threonine-specific protein kinases is involved in many cellular processes, and the unregulated activation of PKC has been implicated in carcinogenesis. PKC inhibitors thus have significant potential as chemotherapeutic agents. Recently, the fungal metabolite balanol was shown to be an exceptionally potent inhibitor of PKC. We previously developed a practical and efficient total synthesis of balanol. We set out to use this synthetic molecule, and several synthetic analogs, to probe the mechanism of PKC inhibition and to determine the effect of balanol on the activity of other protein kinases.

Results: As well as inhibiting PKC, balanol is a potent inhibitor of cyclic AMP-dependent protein kinase (PKA), another protein serine/threonine kinase. Balanol does not, however, inhibit the Src or epidermal growth factor receptor protein tyrosine kinases. The inhibition of

both PKC and PKA by balanol can be overcome by high concentrations of ATP, and molecular modeling studies suggest that balanol may function as an ATP structural analog. Although balanol discriminates rather poorly between PKC and PKA, only minor modifications to its molecular structure are required to furnish compounds that are highly specific inhibitors of PKA.

Conclusions: A number of balanol analogs have been designed and synthesized that, unlike balanol itself, exhibit dramatic selectivity between PKA and PKC. Thus, despite the substantial homology between the catalytic domains of PKA and PKC, there is enough difference to allow for the development of potent and selective inhibitors acting in this region. These inhibitors should be useful tools for analyzing signal transduction pathways and may also aid in the development of drugs with significant therapeutic potential.

Chemistry & Biology September 1995, 2:601–608

Key words: balanol, balanol analogs, inhibitor, protein kinase A, protein kinase C

Introduction

The protein kinase C (PKC) family of enzymes [1–7] catalyzes the transfer of the γ -phosphate from adenosine triphosphate (ATP) to serine or threonine residues on their substrate proteins. PKC-mediated phosphorylation is important in the regulation of a variety of cellular processes, including gene expression and cell proliferation, and the unregulated activation of PKC has been implicated in a number of disease states including carcinogenesis [8]. Intensive efforts have thus been made over the last few years to identify potent and selective inhibitors of PKC. The compound balanol (compound **1**, Fig. 1), a metabolic product of the fungus *Verticillium balanoides*, was recently isolated and found to inhibit PKC in low nanomolar concentrations [9,10]. The recent chemical synthesis of balanol by ourselves [11] and others ([12] and N.Vicker, personal communication) presented us with an opportunity to probe the mechanism of PKC inhibition and to investigate whether balanol could inhibit other protein kinases. Furthermore, through modification of our synthetic strategy, we wished to prepare structurally more simple variants of the natural product [13], with the dual aims of delineating the functional requirements for PKC inhibition and developing novel balanoids with superior activity and selectivity profiles.

Results and discussion

Biological activity of balanol

Synthetic balanol, which was identical to the natural product in all respects [11,13], was used in our biological assays. Balanol was found to be a potent inhibitor of purified rat brain protein kinase C (PKC), with an IC_{50} of 4 nM (Fig. 2a). To determine whether balanol interacted at a known cofactor- or substrate-binding site on PKC, inhibition by balanol was examined in the presence of varying concentrations of histone, diolein, phosphatidylserine or ATP. Thus, the substrate or cofactor concentration was varied over a broad range and PKC activity was assessed in the absence or presence of 10 nM balanol. For histone, diolein and phosphatidylserine the effect of balanol was non-competitive, that is, the inhibitory effect of balanol was observed over the entire concentration range of the variable and was not surmounted by increasing the concentration of the variable component. Only ATP acted competitively with balanol, with high concentrations overcoming the inhibitory effect of balanol to achieve maximal enzyme activity (Fig. 2e). These data are consistent with the findings of Ohshima *et al.* [10] and suggest that balanol and ATP compete for binding to the same site in the catalytic domain of PKC.

*Corresponding authors. L.G.P. is a visiting assistant professor from the University of Naples, Italy.

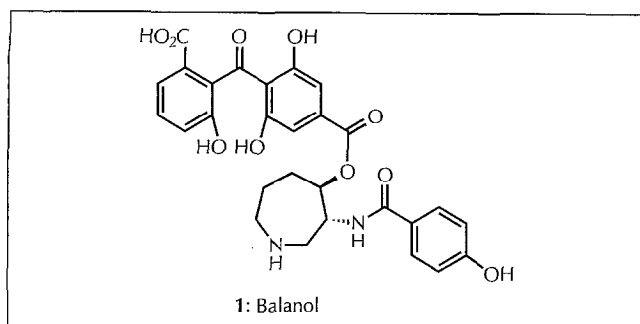


Fig. 1. Molecular structure of balanol (compound 1).

Balanol also inhibited the activity of the catalytic (C) subunit of the cyclic AMP-dependent protein kinase (PKA) [14–21], with an IC_{50} of 4 nM (Fig. 3a), identical to that for inhibition of PKC. The competition profiles were similar to those for PKC. Increasing concentrations of phosphate acceptor did not overcome the effect of balanol (Fig. 3b), whereas ATP at sufficiently high concentrations did (Fig. 3c), implying that balanol was acting competitively with ATP. Results obtained with the purified recombinant C subunit of PKA (cPKA) and with the holoenzyme (purified from rabbit muscle) assayed in the presence of cAMP were similar.

The effectiveness of balanol as an inhibitor of PKA and PKC, both protein serine/threonine kinases, raised the

question of specificity of balanol toward protein kinases in general. We tested balanol against two protein tyrosine kinases, the epidermal growth factor receptor (EGFR) kinase and the Src kinase (pp60 Src). Balanol did not inhibit either of these protein kinase activities, whereas known inhibitors were effective (Fig. 4). Tested against this small number of protein kinases, balanol seems effective against protein serine/threonine kinases and ineffective against protein tyrosine kinases. The effect of balanol on a broader range of protein kinases is currently under investigation.

Molecular modeling studies for balanol

To gain further insight into the action of balanol, and to aid our design of novel balanoids, we generated a structural model of the inhibitor through a combination of conformational analysis (using Monte Carlo methods) and *ab initio* calculations. An initial conformation for balanol (neutral non-zwitterionic form) was constructed using the program Macromodel V3.5X and energy minimized in the MM2 force field (500 steps of energy minimization using a conjugate gradient algorithm). A Monte Carlo conformational search was then performed using a water solvation model [22], allowing complete freedom of movement for all the rotatable bonds to search for the global minimum energy conformation. This conformation was then optimized using the PM3 program contained in the MOPAC software package (128 steps of

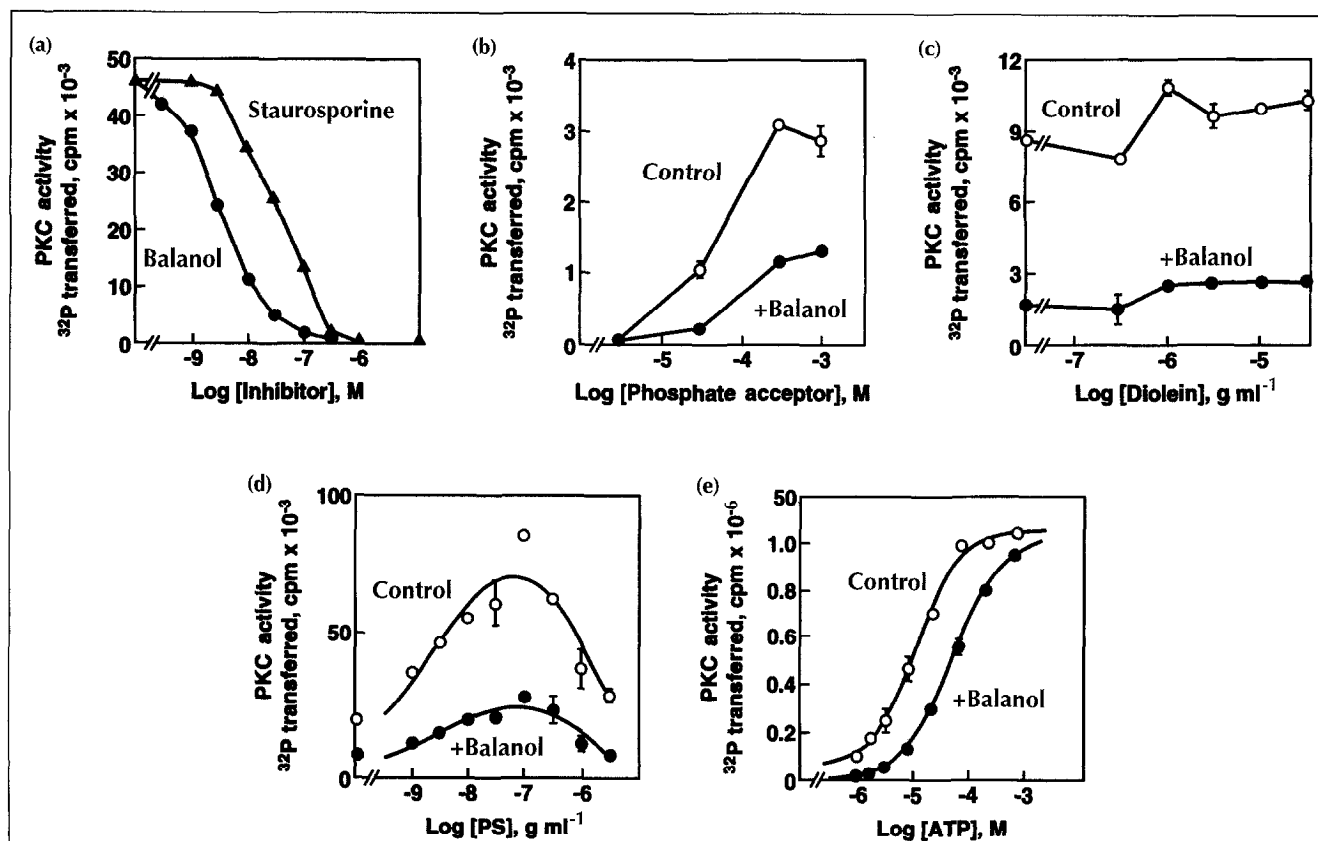
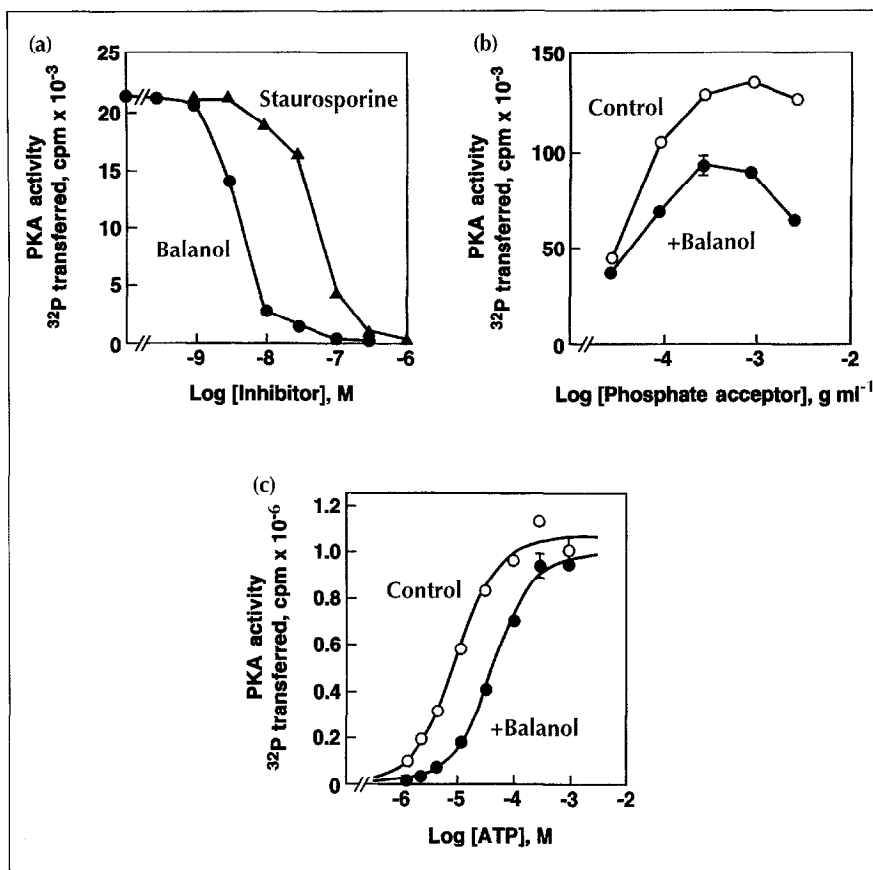


Fig. 2. Inhibition of PKC by balanol can be overcome by high concentrations of ATP. (a) Effect of balanol and staurosporine on PKC activity. (b)–(e) PKC activity assayed in the absence (open circles) or presence (solid circles) of 10 nM balanol as a function of the concentration of (b) peptide substrate, (c) diolein, (d) phosphatidylserine (PS), or (e) ATP. The apparent K_a for ATP is 16 μ M in this experiment and 26 ± 12 μ M in the aggregate (mean \pm standard error measurement (SEM) of three independent determinations).

Fig. 3. Balanol inhibits the activity of cyclic AMP-dependent protein kinase (PKA). **(a)** Effect of balanol and staurosporine on PKA activity. **(b)** & **(c)** PKA activity assayed in the absence (open circles) and presence (solid circles) of 10 nM balanol as a function of the concentration of **(b)** substrate (histone) or **(c)** ATP. The apparent K_a for ATP is 10 μ M in this experiment and 16 ± 7 μ M in the aggregate (mean \pm SEM of four independent determinations).



geometry optimization until the self-consistent field (SCF) gradient was < 0.01 to afford the final balanol model (heat of formation = -325.99 kcal mol⁻¹). The conformation of the central hexahydroazepine ring and the orientation of the benzoyl amide fragment obtained in these modeling studies were completely consistent with the experimental data currently available from ¹H NMR experiments [9]. Furthermore, because of the limited conformational flexibility available to balanol, it is reasonable to suggest that this structural model for balanol (Fig. 5) approximates the conformation involved in protein kinase inhibition.

The active sites of all eukaryotic protein kinases have a high degree of homology [23] and there is increasing evidence for a common mechanism of catalysis for phosphoryl transfer [19]. The structure of the catalytic subunit of PKA (cPKA) has been determined crystallographically [14–21] and may serve as an excellent model for the catalytic domains of other protein serine/threonine kinases such as PKC [24]. We hypothesized that the potent inhibitory properties of balanol might stem from its ability to serve as a structural analog of ATP. The conformation of ATP found in the crystal structure [16,17] of the ternary complex between cPKA, MnATP and a pseudosubstrate peptide corresponding to residues 5–24 of the naturally occurring, heat-stable protein kinase inhibitor (PKI) was compared to that of our balanol model. There is striking similarity in the overall shape and size of the two molecules (Fig. 5). In addition, the oxygen-rich benzophenone domain of balanol closely

correlated with the triphosphate moiety of ATP, and the hydrophobic benzoyl amide fragment correlated with the adenine region. In the structural model of balanol, the central hexahydroazepine ring projects these two key domains in an orientation that is close to that of the corresponding groups in cPKA-bound ATP. The implication that balanol could to some extent mimic ATP was supported by a docking experiment using our structural model of balanol and the ATP-binding region of the cPKA active site (INSIGHT II, v.2.3 software package). This experiment suggested that balanol could fit comfortably in the cleft between the small and large lobes of the catalytic subunit, with the benzoyl amide domain embedded in the hydrophobic pocket. It is important to note that this inhibitor–protein complex did not appear to suffer from any prohibitive van der Waals clashes.

Molecular design of novel balanol analogs

We prepared a number of designed analogs of balanol (Fig. 6) to probe the importance of particular functional groups for inhibitory activity. The syntheses of the designed analogs were carried out by appropriate modification of our chemical synthesis for balanol and are described elsewhere [13].

The benzophenone fragment **2** and hexahydroazepine fragment **3** represent the two halves of the balanol molecule. These analogs were prepared [13] to assess whether the presence of both major domains of balanol is required for activity. The observation that both compounds were ineffective inhibitors ($IC_{50} > 10^{-6}$ M)

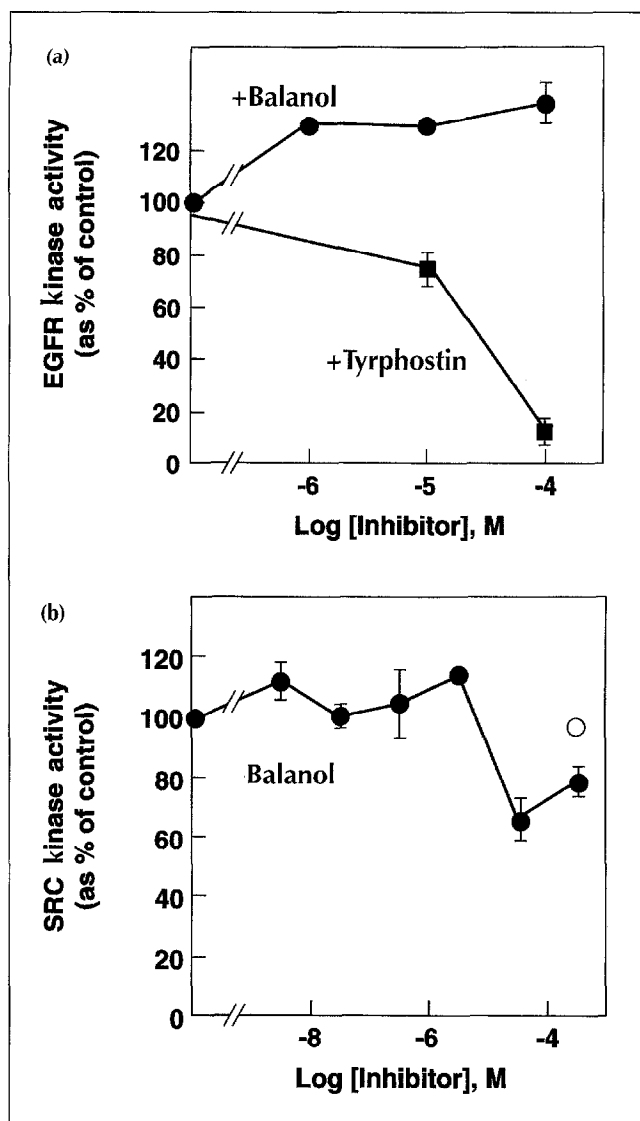


Fig. 4. Balanol does not inhibit protein tyrosine kinases. Activity of (a) EGFR kinase domain or (b) Src kinase in the presence of various concentrations of balanol. The open circle shows the effect of equivalent diluent (30 % DMSO) for the highest concentration of balanol used.

against PKA (Fig. 7a) suggested that the complete balanol backbone should be retained for inhibitory activity. The molecular modeling analysis described above demonstrated that the oxygen-rich benzophenone fragment of balanol could correspond to the triphosphate region of ATP. To examine the importance of this region, the analogs 10"-deoxybalanol (4), 14"-decarboxybalanol (5), and 4",6"-dideoxybalanol (6) were prepared [13]. The binding of the adenine fragment of ATP in the hydrophobic pocket of the cPKA catalytic domain may be stabilized through the formation of a hydrogen bond with the amino moiety [19]. The docking of balanol and cPKA showed that the *p*-hydroxybenzoyl amide fragment may be embedded in this hydrophobic pocket, and the implication that a hydrogen bond with the 5'-hydroxyl moiety of balanol might be important for binding was tested using the 5'-deoxybalanol analog (compound 7).

Biological evaluation of balanol analogs (4–7)

The inhibitory activities of balanol and its analogs 4–7 against PKC and cPKA are shown in Figure 7 and compared in Table 1. Although all of the designed analogs suffered a significant loss of activity for PKC inhibition, a number of them were still potent inhibitors of cPKA. For example, although the decarboxy analog 5 was a poor inhibitor of PKC ($IC_{50} \approx 5 \mu M$), it did not suffer a substantial decrease in potency for inhibition of cPKA ($IC_{50} \approx 18 nM$). Analogs 6 and 7 both inhibited cPKA with IC_{50} values similar to that of balanol (5.5 nM and 5.7 nM, respectively) but were significantly less active as PKC inhibitors ($IC_{50} = 111 nM$ and 95 nM, respectively). The high potency of the decarboxylated analog (7) for inhibition of cPKA suggests that a hydrogen-bonding interaction with the hydrophobic portion of balanol is not essential for binding. The 10"-deoxybalanol analog (4) and the 14"-decarboxybalanol analog (5) exhibited the most dramatic selectivity for cPKA. These analogs were found to be approximately as potent as balanol for the inhibition of cPKA ($IC_{50} = 6.3 nM$ and 18 nM, respectively) but were 125-fold to 1000-fold less effective than balanol against PKC ($IC_{50} \approx 834 nM$ and 6.9 μM , respectively). It is important to note that the inhibition of cPKA by 10"-deoxybalanol (4) also could be overcome by high concentrations of ATP (data not shown), thus confirming that these new balanoids were also acting at the ATP-binding site.

The observation that such minor structural alterations can lead to a marked differentiation in protein kinase selectivity suggests that the binding of balanol at the catalytic

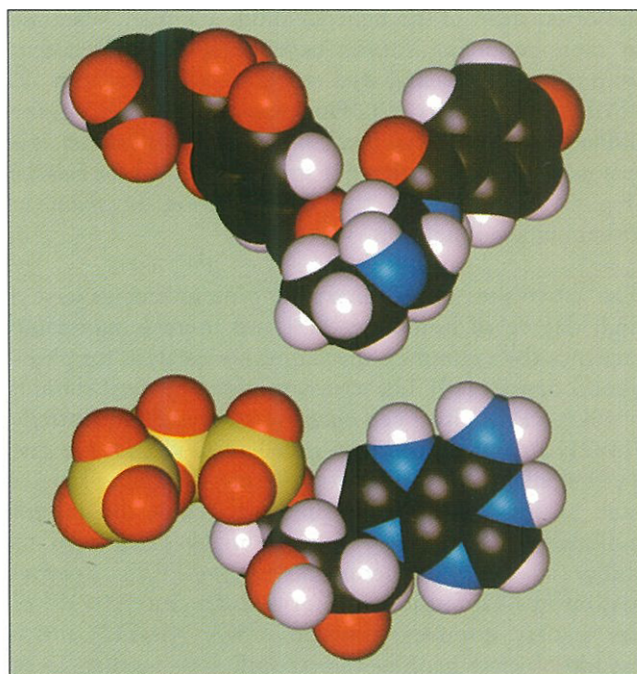
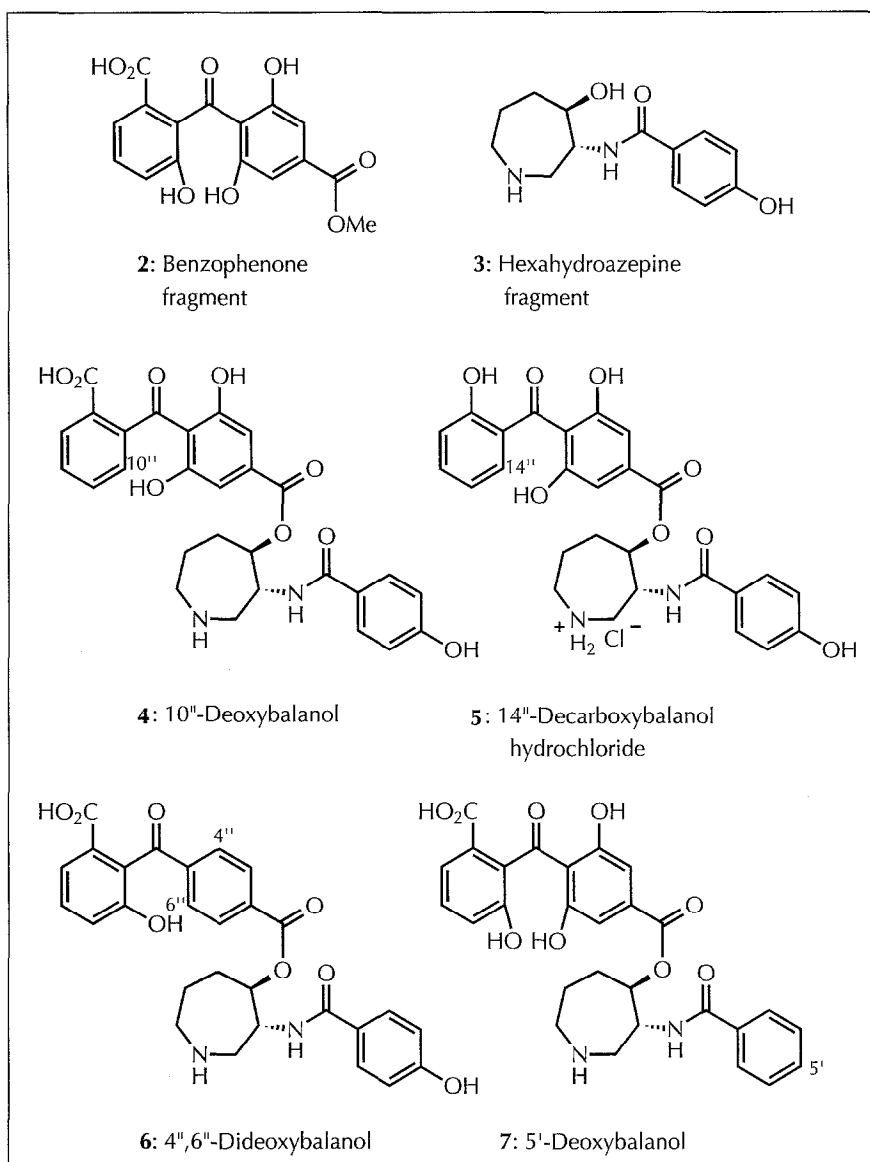


Fig. 5. Comparison of the molecular structures of balanol (above) and the bound conformation of ATP in cPKA (below). Atom colors: carbon, black; hydrogen, white; oxygen, red; nitrogen, blue; phosphorus, yellow. Hydroxyl hydrogen atoms on balanol have been omitted for clarity.

Fig. 6. Molecular structures of designed balanol analogs.

domains of these kinases is more complex than a straightforward mimicking of ATP. These studies also show that, despite the high degree of similarity between the PKA and PKC catalytic domains, they are sufficiently different to allow the development of potent and selective inhibitors which act in the ATP-binding region. The identification of analogs **4** and **5** as selective inhibitors was also of practical interest since their chemical syntheses were much more straightforward than that of balanol itself [13]. To put the above results into perspective, we compared the activity of analogs **4** and **5** to that of the

often-used inhibitor of PKC, staurosporine (compound **8**, Fig. 8). Consistent with previous reports [25], staurosporine was not selective for inhibition of PKC over cPKA and was considerably less potent toward cPKA than either analog or balanol itself (see Table 1). We also compared the inhibitory activity of analogs **4** and **5** with published K_i values for KT5720 (compound **9**, Fig. 8) [26] and H-89 (compound **10**, Fig. 8) [27], two of the most selective non-peptidic inhibitors of PKA reported to date. The novel balanoids **4** and **5** were significantly more potent than these inhibitors against PKA

Table 1. Inhibition constants for balanol derivatives and staurosporine^a.

Kinase	Compound ^b							Staurosporine
	Balanol	(2)	(3)	(4)	(5)	(6)	(7)	
PKA	4.7 ± 1.3	>10 ³	>10 ³	3.9	11	3.4	3.5	35
PKC	5.3 ± 1.8	>10 ⁵	>10 ⁵	640	5000	80	69	19

^a K_i values are shown in nM.

^bSee Figure 6 for the names and structures of compounds 2–7.

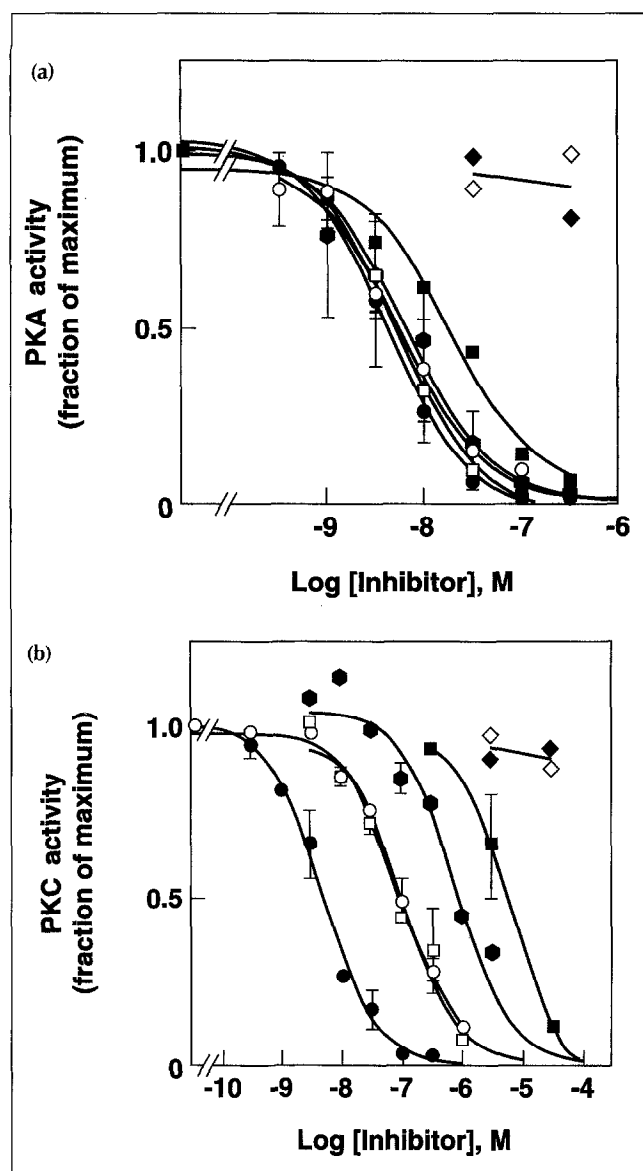


Fig. 7. Comparative effects of balanol analogs on PKC and PKA. The symbols indicate the different analogs (structures are shown in Figs 1 and 6): balanol (1), ●; benzophenone fragment (2), ◆; hexahydroazepine fragment (3), ◇; 10''-deoxybalanol (4), ●; 14''-decarboxybalanol (5), ■; 4'',6''-dideoxybalanol (6), □; 5''-deoxybalanol (7), ○.

and exhibited similar levels of selectivity for PKA compared to PKC (compound 9, $K_i = 56$ nM for PKA; $K_i > 2000$ nM for PKC [26]; compound 10, $K_i = 48$ nM for PKA, $K_i = 31.7$ μ M for PKC [27]).

Significance

The modulation of protein activity through phosphorylation by protein kinases is fundamental to the control of many different cellular events. In particular, the signal transduction pathways that are regulated by PKC and PKA are now highly delineated and it is clear that selective inhibitors of these enzymes could prove therapeutically useful. PKC and PKA are both serine/threonine-specific

protein kinases and have a high degree of homology in their catalytic domains. This homology is presumably reflected in the observation that inhibitors acting at the catalytic domains of these enzymes are generally non-selective (e.g. staurosporine). High enzyme selectivity is, however, essential for any inhibitor to be of value either as a tool for signal transduction research or as a potential drug candidate.

We have shown that the fungal metabolite balanol, originally reported as a PKC inhibitor, also inhibits PKA. Nevertheless, based on molecular modeling studies, a number of new analogs of balanol have been designed and synthesized that show significant selectivity for the inhibition of PKA over PKC. In particular, 10''-deoxybalanol (compound 4) and 14''-decarboxybalanol (compound 5) are remarkably potent and selective inhibitors of PKA. Thus, although the catalytic domains of PKA and PKC show a high degree of homology and probably share a common mechanism for phosphoryl transfer, they are sufficiently different to allow the development of potent and selective inhibitors that act at the ATP-binding region.

Materials and methods

Materials

All of the analogs described here were prepared by chemical synthesis, as described elsewhere [13].

Effects of balanol on activity of PKC

The activity of PKC was assessed by the addition of 10 to 20 ng of purified rat brain PKC (Calbiochem #539494) to a reaction mixture (final volume, 100 μ l) consisting of: 10 μ M ATP, ~ 0.1 μ Ci γ [32 P]ATP, 5 mM $MgCl_2$, 0.5 mM $CaCl_2$, 50 mM Na^+ HEPES, pH 7.5, 100 μ g ml^{-1} phosphatidylserine, 3.3 μ g ml^{-1} diolein, and either 1 mg ml^{-1} histone H1 or 300 μ M peptide substrate (Lys-Arg-Thr-Leu-Arg-Arg; LC Labs #P-3310).

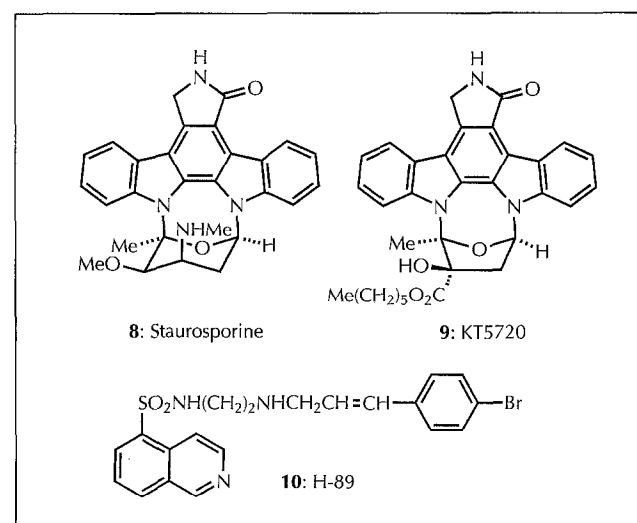


Fig. 8. Structures of staurosporine (compound 8), KT5720 (compound 9) and H-89 (compound 10).

Balanol, its derivatives or diluent were included in these reactions and were added as 10x working stocks diluted with water from stocks made in dimethylsulfoxide (DMSO). DMSO was included as a control and was inactive. Reactions were incubated at 30 °C for 8 min, then 80 µl aliquots were spotted onto phosphocellulose paper (Whatman p81). Papers were washed extensively in 75 mM phosphoric acid and their ³²P content determined by liquid scintillation spectrometry. Each experimental condition was duplicated within each assay. Data presented are the mean ± SEM of two to four experiments.

Effects of balanol on activity of PKA

The activity of PKA was assessed by the addition of 1 to 20 ng of purified recombinant PKA [28] to a reaction mixture (final volume, 100 µl) consisting of: 10 µM ATP, ~0.1 µCi γ[³²P]ATP, 5 mM MgCl₂, 1 mM DTT, 1 mg ml⁻¹ histone Hf2b and 50 mM Na⁺ HEPES, pH 7.5. Reactions were performed and quantified as described above. Data presented are the mean ± SEM of two to four experiments.

Assay of inhibition of protein tyrosine kinases

The activity of the recombinant EGFR kinase domain [29] (gift of Dr Gordon Gill, UC San Diego) was assayed as described [29] using angiotensin II (2 mM) as the phosphate acceptor and 0.1 to 0.5 µg of EGFR kinase per tube. Assays were performed in the presence of increasing concentrations of balanol or tyro-phostin. The activity of Src kinase (10 ng per tube; gift of Dr Tony Hunter, Salk Institute, San Diego) was assayed essentially as described for the EGFR kinase but performed at 30 °C using heat-inactivated enolase (0.2 mg ml⁻¹) as the phosphate acceptor, with reactions terminated by spotting onto Whatman 3MM paper that was subsequently washed extensively with 10 % trichloroacetic acid/2.5 % pyrophosphate. The open circle in Figure 4b shows the effect of equivalent diluent (30 % DMSO) for the highest concentration of balanol used.

Molecular modeling of balanol

All the molecular modeling calculations were performed either on an SGI personal Iris 25G (energy minimizations and Monte Carlo methods) or on a Convex meta cluster C-240 (MOPAC calculations). An initial structural model for balanol was constructed using the program Macromodel 3.1. This conformation was then subjected to energy minimization in the MM2 force field (500 steps using a conjugated gradient algorithm). The balanol conformer obtained by this method was then used as a starting structure for an extensive conformational search by Monte Carlo multiple-minimum calculations [30] using a generalized Born solvent-accessible surface (GB/SA) model [22], in order to locate the global energy minimum. For this purpose a random scan search was performed, allowing all the flexible bonds to rotate in steps randomly chosen over the entire range of 0–360°. The global minimum conformation that was obtained was further refined by *ab initio* calculations at the SCF level [31], using the Hamiltonian PM3 [32] contained in the program MOPAC (QCPE program # 455, available through the Quantum Chemical Program Exchange, QCPE, Department of Chemistry, Indiana University, Bloomington, IN 47405). The structure for ATP was extracted from the ternary complex between cPKA, MnATP, and 5–24 PKI found in the Brookhaven database (structure name: 1atp).

Comparison of the effects of balanol derivatives on PKC and PKA

Balanol and its derivatives were added to reaction mixtures for either PKA or PKC. Assays were conducted as described above.

Data are mean ± SEM for two or three experiments except for balanol (n = 4). Curves were fitted by the program InStat (GraphPad Software, San Diego) using a single component competitive model.

Determination of inhibition constants

K_i values for balanol were estimated in two ways. For the inhibition of kinase activity in the presence varying concentrations of ATP (Figs 2e and 3c), K_i values were determined using the dose-shift method of Cheng and Prusoff [33] in which $[L'/L]-1 = I/K_i$, where L' and L are the concentrations of ATP needed to generate half-maximal kinase activity in the presence or absence of balanol, I is the concentration of inhibitor (balanol, usually 10 nM) and K_i is the apparent inhibition constant for the balanol-kinase interaction. All other K_i values were calculated from the concentration of inhibitor that produced 50 % inhibition of the enzyme activity [the IC₅₀ value, generated by the program InPlot (GraphPad software)], with the assumption that all compounds compete for ATP as demonstrated for balanol and 10"-deoxybalanol. The apparent affinities of ATP for PKC (26 µM) or PKA (16 µM) determined in replicates of the experiments shown in Figures 2c and 3c were used in the calculation. $K_i = [IC_{50} \times K_d] / [L + K_d]$, where IC₅₀ is as above, K_d is the apparent affinity for ATP, and L is the concentration of ATP. Data were derived using determinations from two to four experiments.

Acknowledgements: This work was financially supported by the National Institutes of Health (HL41307 & GN19301), The Scripps Research Institute, UCSD Academic Senate, and the Cancer Research Coordinating Committee of the University of California. M.E.B. thanks the EPSRC, U.K. for a NATO Postdoctoral Fellowship. The authors also thank Dr Sarah Cox for helpful comments.

References

1. Newton, A.C. (1993). Interaction of proteins with lipid headgroups: lessons from protein kinase C. *Annu. Rev. Biophys. Biomol. Struct.* **22**, 1–25.
2. Farago, A. & Nishizuka, Y. (1990). Protein kinase C in transmembrane signalling. *FEBS Lett.* **268**, 350–354.
3. Stabel, S. & Parker, P.J. (1991). Protein kinase C. *Pharmacol. Ther.* **51**, 71–95.
4. Nishizuka, Y. (1984). The role of protein kinase C in cell surface signal transduction and tumor promotion. *Nature* **308**, 693–698.
5. Nishizuka, Y. (1986). Studies and perspectives of protein kinase C. *Science* **233**, 305–312.
6. Nishizuka, Y. (1988). The molecular heterogeneity of protein kinase C and its implications for cellular regulation. *Nature* **334**, 661–665.
7. Nishizuka, Y. (1992). Intracellular signaling by hydrolysis of phospholipids and activation of protein kinase C. *Science* **258**, 607–614.
8. Bradshaw, D., Hill, C.H., Nixon, J.S. & Wilkinson, S.E. (1993). Therapeutic potential of protein kinase C inhibitors. *Agents Actions* **38**, 135–147.
9. Kulanthaivel, P., *et al.*, & Clardy, J. (1993). Balanol: a novel and potent inhibitor of protein kinase C from the fungus *Verticillium balanoides*. *J. Am. Chem. Soc.* **115**, 6452–6453.
10. Ohshima, S., *et al.*, & Okuda, T. (1994). *Fusarium merismoides* Corda NR 6356, the source of the protein kinase C inhibitor, azepinostatin. *J. Antibiot. (Tokyo)* **47**, 639–647.
11. Nicolaou, K.C., Bunnage, M.E. & Koide, K. (1994). Total synthesis of balanol. *J. Am. Chem. Soc.* **116**, 8402–8403.
12. Lampe, J.W., Hughes, P. F., Biggers, C.K., Smith, S.H. & Hu, H. (1994). Total synthesis of (–)-balanol. *J. Org. Chem.* **59**, 5147–5148.
13. Nicolaou, K.C., Koide, K. & Bunnage, M.E. (1995). Total synthesis of balanol and designed analogues. *Chemistry: A European Journal*, in press.
14. Knighton, D.R., *et al.*, & Sowadski, J.M. (1991). Crystal structure of the catalytic subunit of cyclic adenosine monophosphate-dependent protein kinase. *Science* **253**, 407–414.
15. Knighton, D.R., Zheng, J., Ten Eyck, L.F., Xuong, N.-H., Taylor, S.S. & Sowadski, J.M. (1991). Structure of a peptide inhibitor bound to

- the catalytic subunit of cyclic adenosine monophosphate-dependent protein kinase. *Science* **253**, 414–420.
16. Zheng, J., *et al.*, & Sowadski, J.M. (1993). Crystal structure of the catalytic subunit of cAMP-dependent protein kinase complexed with MgATP and peptide inhibitor. *Biochemistry* **32**, 2154–2161.
 17. Zheng, J., *et al.*, & Sowadski, J. M. (1993). 2.2 Å Refined crystal structure of the catalytic subunit of cAMP-dependent protein kinase complexed with MnATP and a peptide inhibitor. *Acta Crystallogr. D* **49**, 362–365.
 18. Zheng, J., Knighton, D.R., Xuong, N.-H., Taylor, S.S., Sowadski, J.M. & Ten Eyck, L.F. (1993). Crystal structures of the myristylated catalytic subunit of cAMP-dependent protein kinase reveal open and closed conformations. *Protein Sci.* **2**, 1559–1573.
 19. Madhusudan, *et al.*, & Sowadski, J. M. (1994). cAMP-dependent protein kinase: crystallographic insights into substrate recognition and phosphotransfer. *Protein Sci.* **3**, 176–187.
 20. Bossenmeyer, D., Engh, R.A., Kinzel, V., Ponstingl, H. & Huber, R. (1993). Phosphotransferase and substrate binding mechanism of the cAMP-dependent protein kinase catalytic subunit from porcine heart as deduced from the 2.0 Å structure of the complex with Mn²⁺ adenylyl imidophosphate and inhibitor peptide PKI(5–24). *EMBO J.* **12**, 849–859.
 21. Taylor, S.S. & Adams, J.A. (1992). Protein kinases: coming of age. *Curr. Opin. Struct. Biol.* **2**, 743–748.
 22. Still, W.C., Tempczyk, A., Hawley, R.C. & Hendrickson, T. (1990). Semianalytical treatment of solvation for molecular mechanics and dynamics. *J. Am. Chem. Soc.* **112**, 6127–6129.
 23. Hanks, S.K., Quinn, A.M. & Hunter, T. (1988). The protein kinase family: conserved features and deduced phylogeny of the catalytic domains. *Science* **241**, 42–51.
 24. Orr, J.W. & Newton, A.C., (1994). Intrapeptide regulation of protein kinase C. *J. Biol. Chem.* **269**, 8383–8387.
 25. Rüegg, U.T. & Burgess, G.M. (1989). Staurosporine, K-252 and UCN-01: potent but nonspecific inhibitors of protein kinases. *Trends Pharm. Sci.* **10**, 218–220.
 26. Kase, H., *et al.*, & Kaneko, M. (1987). K-252 Compounds, novel and potent inhibitors of protein kinase C and cyclic nucleotide-dependent protein kinases. *Biochem. Biophys. Res. Commun.* **142**, 436–440.
 27. Chijiwa, T., *et al.*, & Hidaka, H. (1990). Inhibition of forskolin-induced neurite outgrowth and protein phosphorylation by a newly synthesized selective inhibitor of cyclic AMP-dependent protein kinase, N-[2-(p-bromocinnamylamino)ethyl]-5-isoquinolinesulfonamide (H-89), of PC12D pheochromocytoma cells. *J. Biol. Chem.* **265**, 5267–5272.
 28. Herberg, F.W., Bell, S.M. & Taylor, S.S. (1993). Expression of the catalytic subunit of cAMP-dependent protein kinase in *Escherichia coli*: multiple isozymes reflect different phosphorylation states. *Protein Eng.* **6**, 771–777.
 29. Wedegaertner, P.B. & Gill, G.N. (1989). Activation of the purified protein tyrosine kinase domain of the epidermal growth factor receptor. *J. Biol. Chem.* **264**, 11346–11353.
 30. Chang, G., Guida, W.C. & Still, W.C. (1989). An internal coordinate Monte Carlo method for searching conformational space. *J. Am. Chem. Soc.* **111**, 4379–4386.
 31. Pople, J. & Beveridge, D. L. (1970). *Approximate Molecule Orbital Theory*. McGraw Hill Inc., New York.
 32. Stewart, J.J.P. (1989). Optimization of parameters for semiempirical methods I. Method. *J. Comput. Chem.* **10**, 209–220.
 33. Cheng, Y. & Prusoff, W.H. (1973). Relationship between the inhibition constant (K_i) and the concentration of inhibitor which causes 50% inhibition (I₅₀) of an enzymatic reaction. *Biochem. Pharmacol.* **22**, 3099–3108.

Received: 27 Jul 1995; revisions requested: 11 Aug 1995;
revisions received: 26 Aug 1995. Accepted: 30 Aug 1995.